ON THE USE OF GAUSSIAN FILTER FUNCTIONS FOR ADAPTIVE OPTICS

by

MERFIT ASSAD
B.S. University of Central Florida, 1999

A thesis submitted in partial fulfillment of the requirements
for the degree of Master of Science
in the Department of Mathematics
in the College of Sciences
at the University of Central Florida
Orlando, Florida

Fall Term
2006

ABSTRACT

For adaptive optic systems, the use of aperture filter functions calculated using various Zernike modes can be useful in removing lower-order aberrations caused by atmospheric turbulence. Traditionally, these filter functions are calculated using the step function depicting a hard aperture that introduces integrals that are sometimes difficult to integrate and must be done numerically. The Gaussian method can be used in place of the conventional method for calculating the aperture filter functions.

Evaluation of the Gaussian approximation for modeling a finite receiver aperture can be made by comparison of reduction in phase variance with results achieved using the conventional method. The validity of Gaussian approximation in this application is demonstrated by the consistency of results between the two methodologies.

Comparison of reduction in scintillation by the two methodologies reveals several benefits derived from utilization of Gaussian approximation. The Gaussian approximation produces data that can be interpreted analytically. It further produces greater scintillation reduction.

This paper will first examine the use of statistical models for predicting atmospheric turbulence and then the use of Zernike polynomials in adaptive optics. Next, this paper compares the reduction of phase variance and scintillation using the conventional method with the Gaussian approximation to evaluate the effectiveness of the new filter functions. The results of these comparisons are presented both as mathematical expressions and graphically.

For my beautiful daughter, Jenaan, who inspires me everyday, I dedicate this work in the hope that it may one day inspire her.

ACKNOWLEDGMENTS

"If you help others, you will be helped, perhaps tomorrow, perhaps in one hundred years, but you will be helped. Nature must pay off the debt… It is a mathematical law and all life is mathematics." G.I. Gurdjieff—Nineteenth Century Greek-Armenian Mystic and Spiritual Teacher

This work would not have been possible without the assistance and encouragement of my advisors, colleagues, friends, and family. I extend my sincere appreciation and thanks to my advisors, Larry C. Andrews, Ph.D. and Ram N. Mohapatra, Ph.D. They were the first to encourage me to pursue my graduate degree and provided invaluable guidance in the preparation of this work. And for the many others who took the time to assist in my graduate studies and the presentation of this work, I offer my thanks for your time and encouragement.

TABLE OF CONTENTS

LIST OF FIGURES

LIST OF TABLES

CHAPTER 1
INTRODUCTION

Adaptive optics is a technique used to improve the performance of optical systems by reducing the effects of rapidly changing optical distortion [4]. Astronomical telescopes employ adaptive optics to remove the effects of atmospheric distortion. When light from a star enters the earth's atmosphere, turbulence or random fluctuations distort and move the light image in various ways [4]. The wave arriving from the star is essentially a plane wave before entering the earth's atmosphere. Wave distortion occurs as parts of the wave pass through the hotter-than-average air (less refractive-index) and are advanced [7]. Other parts of the wave are retarded and the plane wave front is deformed. It is the purpose of adaptive optics to compensate for these distortions. A telescope equipped with adaptive optics measures the wave front distortions generated by the variations of the index of refraction in the atmosphere with a wave front sensor and then applies phase corrections with a deformable mirror.

Similar application of adaptive optics can also be used to improve Free-Space Optical (FSO) communication systems that detect optical waves that propagate through the atmosphere. Free-Space Optics (FSO) is a telecommunication technology that uses light propagating in free space to transmit data between two points. The technology is useful where the physical connection of the transmit and receive locations is difficult, for example, in cities where the laying of fiber optic cables is expensive [4]. Other applications for free-space propagation include imaging and laser radar systems. However, the effective use of such technology requires developing an efficient system for resolving wave distortion caused by varying atmospheric conditions.

In the theoretical analysis of optical wave propagation through atmospheric turbulence, the use of aperture filter functions calculated using various Zernike modes can be useful in removing lower-order aberrations caused by atmospheric turbulence. Traditionally, these filter functions are calculated using the step function depicting a hard aperture which introduces integrals which are sometimes difficult to integrate and must be done numerically. The resulting numerical data does not provide analytical results. In this study we investigate the use of a Gaussian approximation for the step function to the receiving aperture and compare results with the conventional approach. First, we will examine the issue of atmospheric turbulence and a theoretical model for predicting turbulence. Next, we will compare the aperture field functions calculated utilizing the conventional approach with the Gaussian method. Our analysis will reveal the benefits of the Gaussian method— greater tractability that leads to analytic results that can provide greater insight.

CHAPTER 2
MODELING ATMOSPHERIC TURBULENCE

Atmospheric turbulence models based upon statistical analysis provide a basis for predicting atmospheric disturbance and scintillation reduction. Such statistical models are used in conjunction with filter functions to achieve phase reduction. The filter functions are based on Zernike modes (Chapter 3) that are traditionally used with a step function depicting a finite size aperture (Chapter 4). In this thesis, we evaluate the use of the Gaussian approximation to the step function which is used in the conventional approach. Once the filter function is established, it can be used with the atmospheric turbulence model to achieve phase reduction (Chapter 7) and scintillation reduction (Chapter 8).

Russian mathematician Andrey Kolmogorov suggested a statistical description of turbulent flow. Atmospheric turbulence is generally described as small-scale, irregular air motions characterized by winds that vary in speed and direction [6]. Other types of atmospheric turbulence include temperature fluctuations and index of refraction fluctuations. Refractive-index variations in the atmosphere produce phase fluctuations in the wave front. Because turbulence is a nonlinear process and is governed by nonlinear equations, Kolmogorov attempted to model turbulence in the atmosphere using a physical or statistical approach.

The Kolmogorov theory of turbulence is based on the assumption that wind velocity fluctuations (classical turbulence) are approximately locally homogeneous and isotropic. Homogenous means that the mean value of the field is constant and other statistical quantities in the field depend only on the separation of points being observed. Isotropic means that the statistical quantities are the same in all directions and depend only on the magnitude of the vector

separation between observation points random fields [1]. Kolmogorov proposed a theory to calculate the energy of such a system.

The energy cascade theory of turbulence provides a tool for visualizing the structure of atmospheric turbulence. Under the cascade theory, the wind velocity increases until a critical Reynolds number is exceeded and turbulence occurs. The resultant turbulence creates "eddies" or unstable air masses which, under the influence of inertial forces, break into smaller eddies which eventually dissipate into heat energy. The largest eddy is referred to as the outer scale L_0 of turbulence and the smallest eddy is the inner scale l_0. Eddies between l_0 and L_0 compose the inertial subrange. This is illustrated in Figure1.

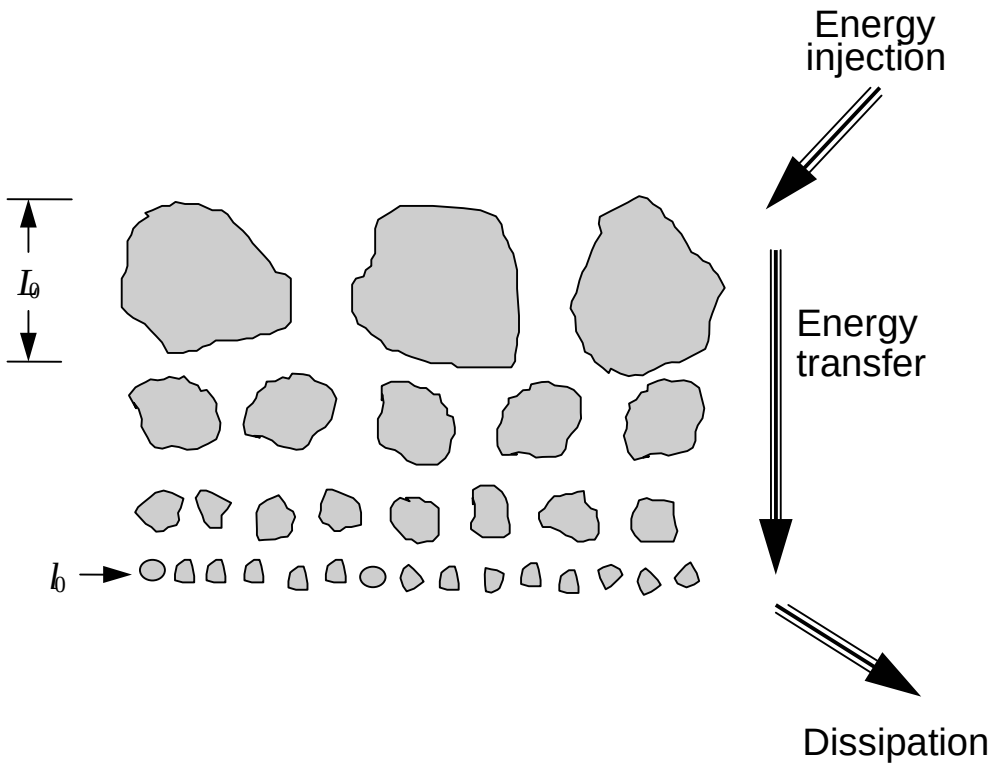

Figure 1 *Large eddies supply energy to the smaller eddies and these in turn supply smaller eddies, resulting in a cascade of energy from the largest to the smallest ones*

Turbulent atmospheric motion due to the presence of moisture and temperature gradients gives rise to disturbances in the atmosphere's refractive-index $n(\mathbf{R})$,where $\mathbf{R}$ is a vector and $|\mathbf{R}| = R$ is distance between two points. We define these disturbances in the index of refraction as optical turbulence [1].

Refractive-index variations in the atmosphere produce phase fluctuations in the wave front. The index of refraction is one of the most significant parameters of the atmosphere for optical wave propagation. It is very sensitive to small-scale temperature fluctuations [1]. It is not realistic to measure the instantaneous three-dimensional turbulent structure in the atmosphere [8]. Therefore, we must rely on a statistical analysis.

The statistical description or structure of fluctuations in the refractive-index of the atmosphere is very similar to that for the field of turbulent velocities. The inertial subrange is statistically homogenous and isotropic. The structure function $D_n(R)$ given in (1) is a spatial description of optical turbulence and is given by

$$D_n(R) = < n_1 - n_2 > = C_n^2 R^{2/3}, \quad l_0 \ll R \ll L_0 \tag{1}$$

where C_n^2 is the index of refraction structure constant (in units of $m^{-2/3}$) or a measure of the strength of the fluctuations in the refractive-index. The $< \quad >$ symbol denotes the statistical average.

For optical wave propagation, fluctuations in the index of refraction are primarily caused by small fluctuations in temperature. The functional form of the spatial power spectrum of refractive-index fluctuations is the same as that for temperature. In addition, temperature fluctuations obey the same spectral laws as velocity [1].

The spatial power spectrum is a description in terms of wave number. Based on the $2/3$ power law behavior of the structure function (1) in the inertial subrange, the Kolmogorov spatial power spectrum model $\phi_n(\kappa)$ for the index of refraction is

$$\phi_n(\kappa) = 0.033 C_n^2 \kappa^{-\frac{11}{3}}, \quad \frac{1}{L_0} \leq \kappa \leq \frac{1}{l_0} \tag{2}$$

where κ is wave number.

The Kolmogorov power-law spectrum is commonly used in theoretical calculations. However, this spectrum model is valid only over the inertial subrange $\frac{1}{L_0} \leq \kappa \leq \frac{1}{l_0}$. In order to justify the use of the Kolmogorov power-law spectrum in calculations over all wave numbers, it is assumed that the outer scale is infinite $(L_0 = \infty)$ and the inner scale is negligibly small $(l_0 = 0)$. However, this may lead to divergent integrals. Therefore, other spectrum models have been used when inner scale and outer scale effects cannot be ignored. These spectrum models are often modified so that the turbulence is modeled as if it were statistically homogenous and isotropic for all wave numbers. One of those spectrum models which includes both inner scale and outer scale effects is the modified von Karman spectrum which is defined as

$$\phi_n(\kappa) = 0.033 C_n^2 \frac{e^{-\frac{\kappa^2}{\kappa_m^2}}}{(\kappa^2 + \kappa_0^2)^{\frac{11}{6}}}, \quad 0 \leq \kappa < \infty \tag{3}$$

where $\kappa_0 = \frac{1}{L_0}$ and $\kappa_m = \frac{1}{l_0}$.

CHAPTER 3
ZERNIKE POLYNOMIALS $Z_i(r,\theta)$

The Zernike polynomials were originally used to represent fixed aberrations in optical systems, but are now also used in adaptive optics systems designed for atmospheric turbulence decomposition. The Zernike polynomials represent a set of functions of two variables that are orthogonal over a circle with unit radius. These polynomials are the product of two functions, one depending only on a radial coordinate r and the other depending only on the angular coordinate θ, i.e.,

$$Z_n^m(r,\theta) = R_n^m(r)e^{im\theta} \tag{4}$$

where both m and n are integers, $n \geq 0$, $-n \leq m \leq n$, and $n \pm |m|$ is even. The angular functions are the basis functions for the two-dimensional rotation group, and the radial polynomials are a special case of Jacobi or hypergeometric polynomial that are normalized so that $R_n^m(1) = 1$. It is defined by

$$R_n^m(r) = \sum_{k=0}^{(n-|m|)/2} \frac{(-1)^k (n-k)!}{\left(\frac{n+m}{2}-k\right)!\left(\frac{n-m}{2}-k\right)!} r^{n-2k} \tag{5}$$

In the theoretical analysis of adaptive optics systems the Zernike polynomials are normalized over a unit radius aperture so that

$$\frac{1}{\pi}\int_0^{\infty}\int_0^{2\pi} rU(1-r)Z_i^{\,2}(r,\theta)d\theta dr = 1, \quad i = 1,2,3 \tag{6}$$

where we define

$$\begin{aligned} Z_i(r,\theta) &= Z_i[0,n] = \sqrt{n+1}R_n^{\,0}(r),\ m = 0 \\ Z_i(r,\theta) &= Z_i[m,n] = \sqrt{n+1}R_n^{\,m}(r)\sqrt{2}\cos m\theta,\ i\ even\ (m \neq 0) \\ Z_i(r,\theta) &= Z_i[m,n] = \sqrt{n+1}R_n^{\,m}(r)\sqrt{2}\sin m\theta,\ i\ odd\ (m \neq 0) \end{aligned} \tag{7}$$

and where $U(1-r)$ is the step function defined by

$$U(1-r) = \begin{cases} 1, 0 \le r < 1 \\ 0, r > 1 \end{cases} \tag{8}$$

Using this definition, the first 6 Zernike polynomials are given in Table 1. They are arranged by (m,n) pair and indexed by i. Table 1 contains all the Zernike polynomials through $(m,n) = (2,2)$. Note that for cases where $m > 0$ there are two Zernike polynomials for each (m,n) pair which represent the x and y components (of the Zernike mode).

Table 1 Zernike polynomials for hard aperture

i	m	n	Zernike Polynomial $Z_i[m,n]$	Description
1	0	0	1	Piston
2	1	1	$2r\cos\theta$	Tilt about *x axis*
3	1	1	$2r\sin\theta$	Tilt about *y axis*
4	0	2	$\sqrt{3}(2r^2-1)$	Defocus
5	2	2	$\sqrt{6}r^2\sin 2\theta$	Astigmatism
6	2	2	$\sqrt{6}r^2\cos 2\theta$	Astigmatism

The Zernike polynomials given in Table 1 are a modification of the Zernike polynomials that are commonly used in studying atmospheric effects on imaging systems. Each term of the Zernike polynomials minimize the residual mean square (rms) wave front error to the order of that term. The first Zernike mode, $Z_1[0,0]$, is referred to as piston. Physically, piston corresponds to the aperture averaged wave front phase. The Zernike modes $Z_2[1,1]$ and $Z_3[1,1]$ are referred to as tilt. Tilt does not affect image quality, but does cause the image to be displaced. Other Zernike modes with well known names include $Z_4[0,2]$, which is called defocus; and $Z_5[2,2]$ and $Z_6[2,2]$ which are the orthogonal components of astigmatism.

CHAPTER 4
APERTURE FIELD FILTER FUNCTIONS $G_i(\kappa,\phi)$: CONVENTIONAL APPROACH

4.1 Normalized Zernike Polynomials

The Zernike polynomials appearing in Table 1 are already normalized to satisfy the condition on the unit circle given by (6).

4.2 Calculation of Filter Functions

The two-dimensional Fourier transform of the Zernike polynomials, scaled by the area of the aperture, is given by

$$\begin{aligned} G_i(\kappa,\phi) &= \frac{1}{\pi}\int_{-\infty}^{\infty}\int_{-\infty}^{\infty} e^{i\mathbf{r}\cdot\mathbf{k}} Z_i(r,\theta)U(1-|r|)dxdy \\ &= \frac{1}{\pi}\int_{0}^{1}\int_{0}^{2\pi} e^{ir\kappa\cos(\theta-\phi)} Z_i(r,\theta)rd\theta dr \end{aligned} \tag{9}$$

where $\mathbf{r} =< x, y >$ and $\boldsymbol{\kappa} =< \kappa_x, \kappa_y >$ are two-dimensional vectors in the spatial and wave number domains, respectively. $U(x)$ is the step function depicting the finite size of the aperture. In (9) $G_i(\kappa,\phi)$ reduces down using

$$\mathbf{r}\cdot\boldsymbol{\kappa} = x\kappa_x + y\kappa_y = r\kappa\cos(\theta-\phi) \tag{10}$$

since

$$\begin{aligned} x &= r\cos\theta, \quad \kappa_x = \kappa\cos\theta \\ y &= r\sin\theta, \quad \kappa_y = \kappa\sin\theta \end{aligned} \tag{11}$$

Substituting the Zernike polynomials into (9), we obtain

$$\left.\begin{matrix} G_i(\kappa) \\ G_{i,even}(\kappa,\phi) \\ G_{i,odd}(\kappa,\phi) \end{matrix}\right\} = \frac{\sqrt{n+1}}{\pi}\int_0^1\int_0^{2\pi} e^{i\kappa r\cos(\theta-\phi)} r R_n^m(r) \left\{\begin{matrix} 1 \\ \sqrt{2}\cos m\theta \\ \sqrt{2}\sin m\theta \end{matrix}\right\} d\theta dr \tag{12}$$

Filter 1:

We will calculate the first few filter functions using the conventional approach. To compute the aperture filter function corresponding to piston we substitute $m = 0$ and $R_0^0(r) = 1$ or $Z_1[0,0] = 1$ into the integral above. From this we have

$$G_1(\kappa) = \frac{1}{\pi}\int_0^1 r\int_0^{2\pi} e^{ir\kappa\cos(\theta-\phi)} d\theta dr = 2\int_0^1 r J_0(\kappa r) dr\,, \tag{13}$$

or, upon evaluation,

$$G_1(\kappa) = 2\frac{J_1(\kappa)}{\kappa} \tag{14}$$

where $J_n(\kappa)$ is the Bessel function of first kind of order n.

Filter 2:

For the case of tilt corresponding to $Z_2[1,1] = 2r\cos\theta$, substituting into (12) gives us

$$G_{2,even}(\kappa,\phi) = \frac{2}{\pi}\int_0^1 r^2 \int_0^{2\pi} e^{ir\kappa\cos(\theta-\phi)}\cos\theta d\theta dr \tag{15}$$

To evaluate the inside integral in(15), we use the identity

$$e^{ir\kappa\cos(\theta-\phi)} = J_0(\kappa r) + 2\sum_{k=0}^{\infty} i^k J_k(\kappa r)\cos k(\theta-\phi) \tag{16}$$

from which we obtain

$$\begin{aligned}\int_0^{2\pi} e^{ir\kappa\cos(\theta-\phi)}\cos\theta d\theta &= \int_0^{2\pi} J_0(\kappa r)\cos\theta d\theta + \int_0^{2\pi} 2\sum_{k=0}^{\infty} i^k J_k(\kappa r)\cos k(\theta-\phi)\cos\theta d\theta \\ &= J_0(\kappa r)\int_0^{2\pi}\cos\theta d\theta + 2\sum_{k=0}^{\infty} i^k J_k(\kappa r)\cos k\phi\int_0^{2\pi}\cos k\theta\cos\theta d\theta \\ &\quad + 2\sum_{k=0}^{\infty} i^k J_k(\kappa r)\sin k\phi\int_0^{2\pi}\sin k\theta\cos\theta d\theta\end{aligned} \tag{17}$$

and hence

$$\int_0^{2\pi} e^{ir\kappa\cos(\theta-\phi)}\cos\theta d\theta = 2\pi i J_1(\kappa r)\cos\phi \tag{18}$$

The integral in (15) reduces to

$$\begin{aligned} G_{2,even}(\kappa,\phi) &= 4i\cos\phi\int_0^1 r^2 J_1(\kappa r)dr \\ &= 4i\frac{J_2(\kappa)}{\kappa}\cos\phi \end{aligned} \tag{19}$$

The remaining filters can be calculated in a similar manner. It has been shown that the aperture filter functions in the general case are given by

$$\left.\begin{matrix} G_i(\kappa) \\ G_{i,even}(\kappa,\phi) \\ G_{i,odd}(\kappa,\phi) \end{matrix}\right\} = \sqrt{n+1}\frac{2J_{n+1}(\kappa)}{\kappa}\left\{\begin{matrix} (-1)^{n/2} \\ (-1)^{(n-m)/2}\sqrt{2}i^m\cos m\phi \\ (-1)^{(n-m)/2}\sqrt{2}i^m\sin m\phi \end{matrix}\right\} \tag{20}$$

The values of m and n are determined by the choice of Zernike polynomial given in Table 1.

CHAPTER 5
APERTURE FIELD FILTER FUNCTIONS $G_i(\kappa,\phi)$: GAUSSIAN APPROACH

The step function $U(x)$ introduces a Bessel function in the $G_i(\kappa,\phi)$ which is difficult to use in the theoretical analysis of wave front aberrations and consequently are handled by numerical analysis only. Rather than using a hard aperture or a finite size of the aperture of radius 1, we can use a Gaussian approximation $U(1-|r|) \approx 2e^{-2r^2}$ (see Figure 2).

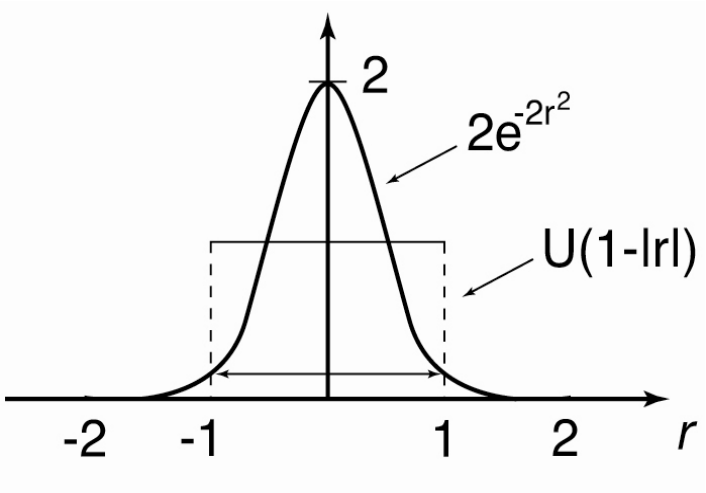

Figure 2 *Gaussian Approximation* $U(1-|r|) \approx 2e^{-2r^2}$

We arrive at this by first assuming

$$U(1-|r|) \approx Ae^{-\alpha r^2} \tag{21}$$

where the constants A and α must be determined. Since $\frac{1}{e^2} = radius$, we have $\alpha = 2$. Integrating both sides we have

$$\int_0^{2\pi}\int_0^{\infty} rU(1-|r|)drd\theta = A\int_0^{2\pi}\int_0^{\infty} re^{-2r^2}drd\theta = \frac{\pi A}{2} \tag{22}$$

Hence, based on the equivalent area under the step function value, we set $A = 2$. In this case the filter function is defined by

$$G_i(\kappa,\phi) = \frac{1}{\pi}\int_0^{\infty}\int_0^{2\pi} e^{ir\kappa\cos(\theta-\phi)}Z_i(r,\theta)2e^{-2r^2}rd\theta dr \tag{23}$$

5.1 Normalized Zernike Polynomials

The Zernike polynomials appearing in (9) must be normalized differently when using the Gaussian approximation so that the normalizations satisfy a condition on the unit circle similar to that given by (6) where $U(1-r)$ is replaced by $2e^{-2r^2}$. Using the definition of the Zernike polynomials given in Table 1, the normalization found here is defined by

$$C_i = \frac{2}{\pi}\int_0^{\infty}\int_0^{2\pi} re^{-2r^2}Z_i^{\,2}(r,\theta)d\theta dr, \quad i = 1,2,3,... \tag{24}$$

where C_i is not necessarily unity. We introduce a multiplicative constant A_i in each polynomial so that $C_i = 1, i = 1,2,3....$ The first Zernike polynomial is simply a constant. For $Z_1[0,0] = A_1$, we find

$$C_1 = \frac{2}{\pi}\int_0^{\infty}\int_0^{2\pi} re^{-2r^2}(A_1)^2 d\theta dr$$
$$= 4(A_1)^2\int_0^{\infty} re^{-2r^2} dr = (A_1)^2$$

from which we deduce $A_1 = 1$. For $Z_2[1,1] = 2A_2 r\cos\theta$, we get

$$C_2 = \frac{2}{\pi}\int_0^{\infty}\int_0^{2\pi} re^{-2r^2}(2A_2 r\cos\theta)^2 d\theta dr$$
$$= \frac{2(A_2)^2}{\pi}\int_0^{\infty} r(4r^2)e^{-2r^2} dr\int_0^{2\pi}\cos^2\theta d\theta$$
$$= 8(A_2)^2\int_0^{\infty} r^3 e^{-2r^2} dr = (A_2)^2$$

and conclude $A_2 = 1$. For $i = 3,4,5,6$ we obtain the normalized Zernike polynomials for the Gaussian aperture. These are listed in Table 2 (see Appendix A for details).

Table 2 Zernike polynomials for Gaussian approximation

i	m	n	Zernike Polynomial $Z_i[m,n]$	Description
1	0	0	1	Piston
2	1	1	$2r\cos\theta$	Tilt about *x axis*
3	1	1	$2r\sin\theta$	Tilt about *y axis*
4	0	2	$2r^2-1$	Defocus
5	2	2	$2r^2\sin 2\theta$	Astigmatism
6	2	2	$2r^2\cos 2\theta$	Astigmatism

5.2 Calculation of Filter Functions

In this section, we illustrate the development of several filter functions. The others can be developed in a similar manner.

Filter 1:

The first aperture filter function is defined by

$$G_1(\kappa,\phi)=\frac{2}{\pi}\int_0^{\infty}\int_0^{2\pi} e^{ir\kappa\cos(\theta-\phi)}Z_1(r,\theta)e^{-2r^2}rd\theta dr \qquad (25)$$

The associated Zernike polynomial is $Z_1[0,0]=1$ which represents piston. Evaluating the inside integral(25), we obtain

$$\int_0^{2\pi} e^{ir\kappa\cos(\theta-\phi)}d\theta = 2\pi J_0(\kappa r) \tag{26}$$

Then

$$G_1(\kappa,\phi) \equiv G_1(\kappa) = 4\int_0^{\infty} re^{-2r^2} J_0(\kappa r)dr \tag{27}$$

which simplifies to (see Appendix A)

$$G_1(\kappa) = e^{-\frac{\kappa^2}{8}} \tag{28}$$

The filter function given by (27) is for an aperture of radius one. Converting to an arbitrary size aperture diameter D, we can simply replace κ by $\frac{\kappa D}{2}$, from which we obtain

$$G_1(\kappa) = e^{-\frac{\kappa^2 D^2}{32}} \tag{29}$$

Filter 2:

The second filter is computed similarly and is used to remove tilt. It is defined by

$$G_2(\kappa,\phi) = \frac{2}{\pi}\int_0^{\infty}\int_0^{2\pi} e^{ir\kappa\cos(\theta-\phi)} Z_2(r,\theta) e^{-2r^2} r\,d\theta\,dr$$
$$= \frac{4}{\pi}\int_0^{\infty}\int_0^{2\pi} e^{ir\kappa\cos(\theta-\phi)} r\cos\theta e^{-2r^2} r\,d\theta\,dr \tag{30}$$

If we use the identity

$$e^{ir\kappa\cos(\theta-\phi)} = J_0(\kappa r) + 2\sum_{k=0}^{\infty} i^k J_k(\kappa r)\cos k(\theta-\phi) \tag{31}$$

then the inside integral in (30) becomes

$$\int_0^{2\pi} e^{ir\kappa\cos(\theta-\phi)}(\cos\theta)d\theta = \int_0^{2\pi}\left[J_0(\kappa r) + 2\sum_{k=0}^{\infty} i^k J_k(\kappa r)\cos\kappa(\theta-\phi)\right]\cos\theta\,d\theta$$
$$= 2\pi i J_1(\kappa r)\cos\phi \tag{32}$$

Hence, (30) reduces to

$$G_2(\kappa,\phi) = \frac{8\pi i}{\pi}\int_0^{\infty} r^2 e^{-2r^2} J_1(\kappa r)\cos\phi\,dr \tag{33}$$

Upon evaluation, we are led to (see Appendix A)

$$G_2(\kappa,\phi) = \frac{i\kappa}{2} e^{-\frac{\kappa^2}{8}}\cos\phi \tag{34}$$

There is also a similar y component for tilt given by

$$G_3(\kappa,\phi) = \frac{i\kappa}{2} e^{-\frac{\kappa^2}{8}} \sin\phi \qquad (35)$$

Recall the corresponding filter functions from (20) are

$$G_1(\kappa) = \frac{2J_1(\kappa)}{\kappa} \qquad (36)$$

$$G_2(\kappa) = \frac{4J_2(\kappa) i \cos m\phi}{\kappa} \qquad (37)$$

and

$$G_3(\kappa) = \frac{4J_2(\kappa) i \sin m\phi}{\kappa} \qquad (38)$$

CHAPTER 6
APERTURE FILTER FUNCTIONS $F_i(\kappa,\phi)$

The $G_i(\kappa)'s$ are "field filters" for the removal of the Zernike modes. For phase and intensity variances, the magnitude squared of the field filters is needed. The filter functions that we need for atmospheric effects are certain combinations of the squared magnitude of the $G_i(\kappa)$ filters defined by

$$F_i(\kappa) = \left|G_i(\kappa)\right|^2 \tag{39}$$

However, because piston corresponds to $i = 1$ and tilt components include $i = 2,3$ we will adopt the notation $F_{piston}(\kappa)$, $F_{tilt}(\kappa)$ and so on to avoid confusion. In the analysis below, we will derive these filter functions based on the Gaussian approach. The comparable filter functions based on the conventional approach will be summarized below in Table 3.

6.1 Aperture Filter Function

The first filter corresponding to the piston mode of the Zernike polynomials is given by

$$F_{piston}(\kappa) \equiv F_1(\kappa) = \left|G_1(\kappa)\right|^2 \tag{40}$$

or, using (28),

$$F_{piston}(\kappa) = e^{-\frac{\kappa^2 D^2}{16}} \tag{41}$$

Since tilt has both an x and y component, we sum the corresponding filters to find

$$\begin{aligned} F_{tilt}(\kappa) &= F_2(\kappa) + F_3(\kappa) \\ &= \left|G_2(\kappa)\right|^2 + \left|G_3(\kappa)\right|^2 \end{aligned} \tag{42}$$

which leads to

$$F_{tilt}(\kappa) = \frac{\kappa^2 D^2}{16} e^{-\frac{\kappa^2 D^2}{16}} \tag{43}$$

In a similar manner, we find

$$F_{focus}(\kappa) = \left|G_4\left(\kappa\right)\right|^2 = \frac{\kappa^4 D^2}{1024} e^{-\frac{\kappa^2 D^2}{16}} \tag{44}$$

and

$$F_{astigmatism}(\kappa) = \left|G_5(\kappa)\right|^2 + \left|G_6(\kappa)\right|^2 = \frac{\kappa^4 D^2}{1024} e^{-\frac{\kappa^2 D^2}{16}} \tag{45}$$

Note that as a consequence that the Zernike polynomials for focus and astigmatism are all quadratic in r, the resulting filter functions (44) and (45) are the same. The aperture filter

functions derived using the Gaussian approach are listed in Table 3 below along with the corresponding filter functions found using the conventional approach.

Table 3 Comparison of Aperture Filter Functions

Filter	Conventional	Gaussian
$F_{piston}(\kappa)$	$16\left[\frac{J_1(\kappa D/2)}{\kappa D}\right]^2$	$e^{-\frac{\kappa^2 D^2}{16}}$
$F_{tilt}(\kappa)$	$64\left[\frac{J_2(\kappa D/2)}{\kappa D}\right]^2$	$\frac{\kappa^2 D^2}{16} e^{-\frac{\kappa^2 D^2}{16}}$
$F_{focus}(\kappa)$	$48\left[\frac{J_3(\kappa D/2)}{\kappa D}\right]^2$	$\frac{\kappa^4 D^2}{1024} e^{-\frac{\kappa^2 D^2}{16}}$
$F_{astigmatism}(\kappa)$	$96\left[\frac{J_3(\kappa D/2)}{\kappa D}\right]^2$	$\frac{\kappa^4 D^2}{1024} e^{-\frac{\kappa^2 D^2}{16}}$

6.2 Graphical Results of Filter Functions

For a graphical representation of the aperture filter functions, refer to Figures 3 - 6. For the purpose of comparison, $D = 1$ was chosen. The curve for Filter 1 derived using the Gaussian approach matches closely to the curve for Filter 1 obtained using the conventional approach (see Figure 3). The curve for Filter 2 derived using the Gaussian approach starts to differ from that of the curve for Filter 2 obtained using the conventional approach. There is a more apparent difference between the filters for the focus mode. As we move to higher-order modes, the difference between the conventional filter and the Gaussian filter is greater as illustrated in Figure 6 where the astigmatism mode shows the largest difference. However, when using these filters to predict phase and scintillation variance, the integration will create a smoothing effect for the Gaussian function.

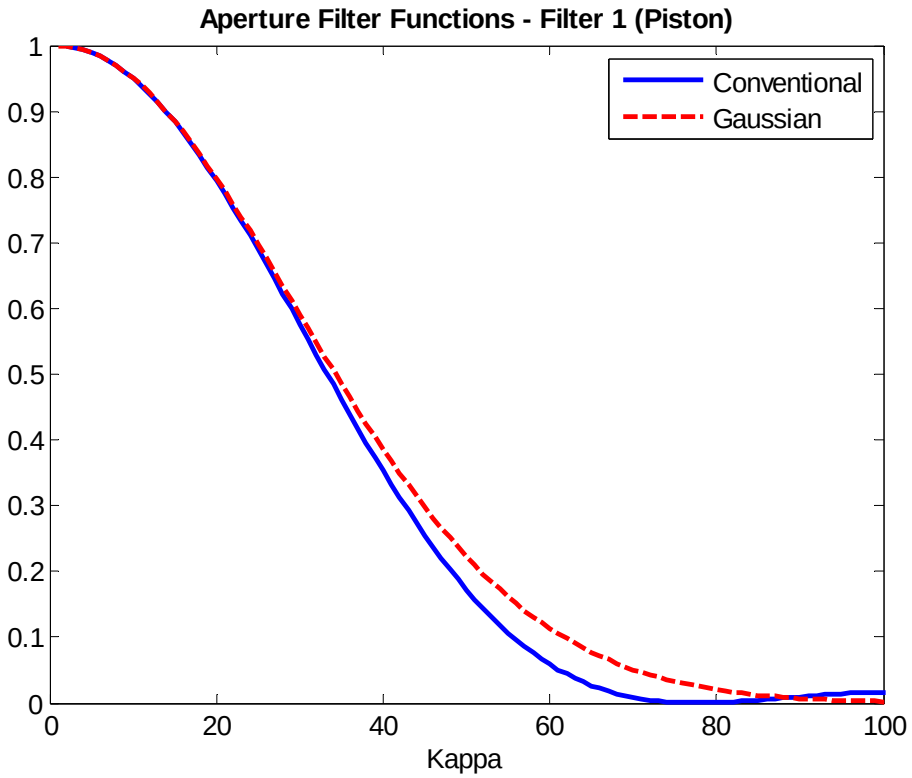

Figure 3 *Graphical comparison of Filter 1 using the conventional filter and its Gaussian approximation*

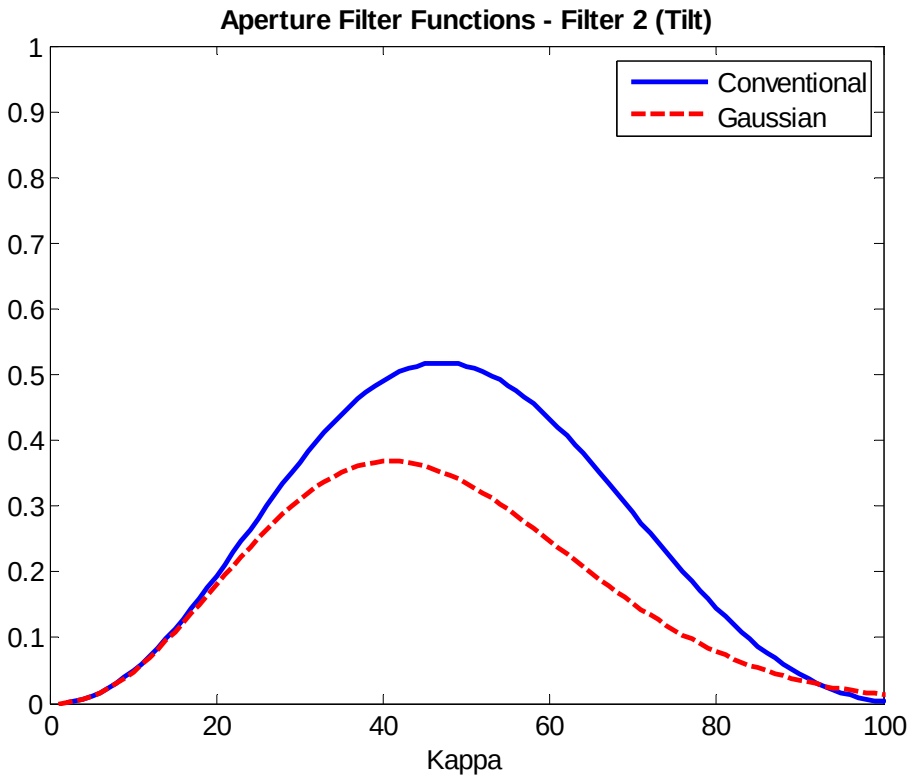

Figure 4 *Same as Figure 3 for Filter 2*

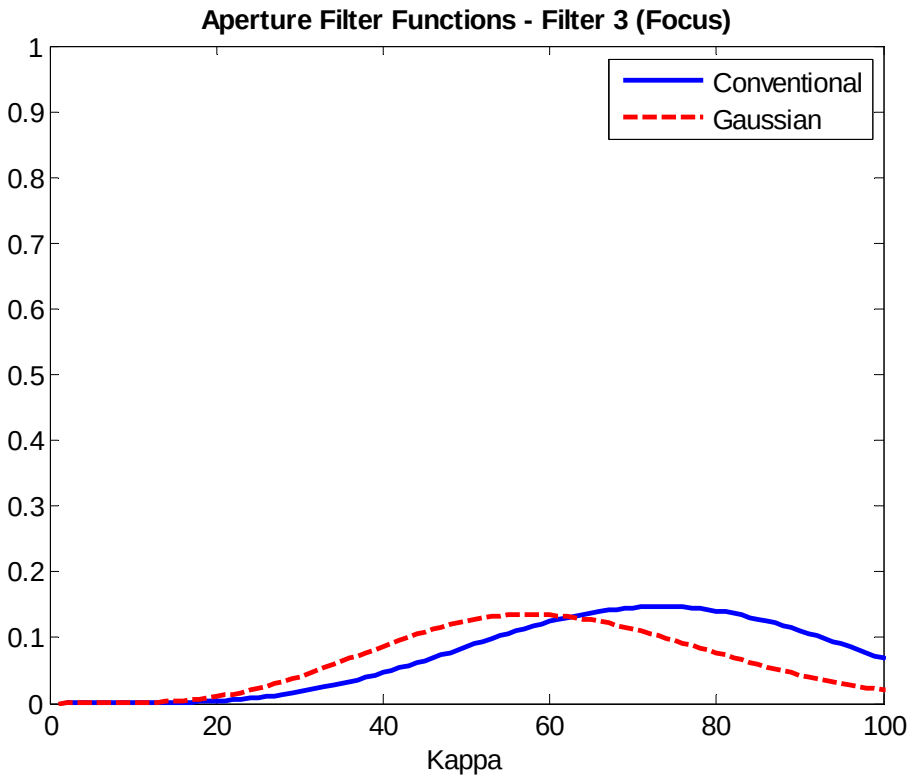

Figure 5 *Same as Figure 3 for Filter 3*

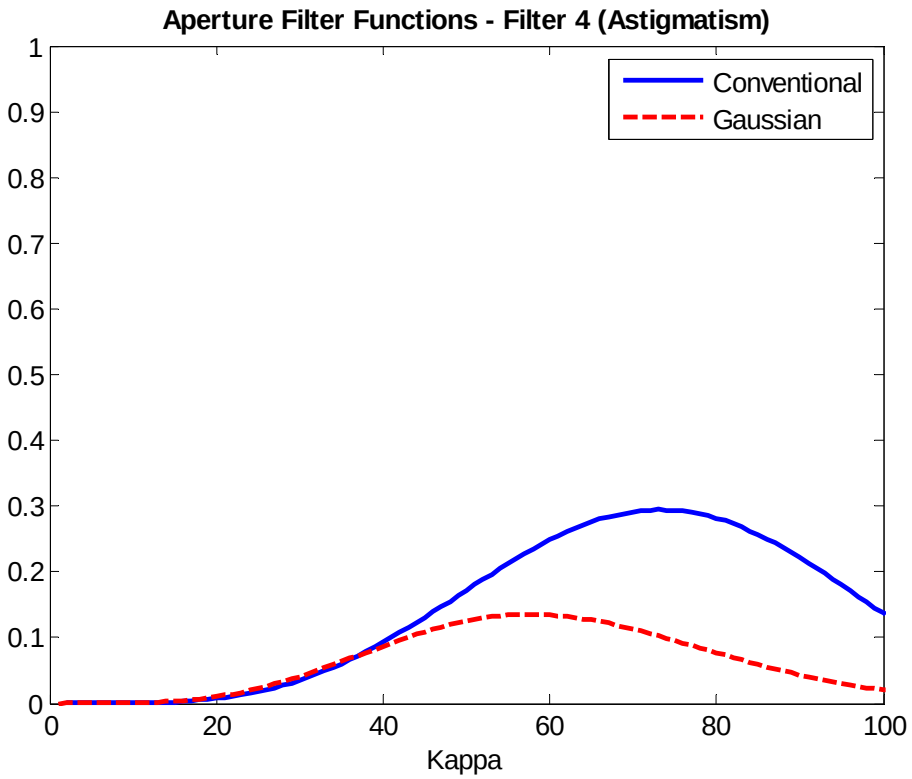

Figure 6 *Same as Figure 3 for Filter 4*

CHAPTER 7
PHASE VARIANCE $\sigma_s^2(L)$

The phase front is a surface of constant phase. For an infinite plane wave the phase front stays planar as the wave propagates in a vacuum. In the atmosphere, however, the phase front becomes distorted in a random fashion. The variance of such a phase front at a single point in the receiver plane based on a geometrical optics approximation is

$$\sigma_s^2 = 4\pi^2 k^2 \int_0^L \int_0^\infty \kappa \phi_n(\kappa) d\kappa dz \tag{46}$$

where $\phi_n(\kappa)$ is the atmospheric power spectrum.

For the Kolmogorov spectrum, the integral in (46) diverges because of the singularity at $\kappa = 0$. Hence to evaluate (46), we use the von Karman spectrum

$$\phi_n(\kappa) = \frac{0.033 C_n^2 e^{-\frac{\kappa^2}{\kappa_m^2}}}{\left(\kappa^2 + \kappa_0^2\right)^{\frac{11}{6}}}, \tag{47}$$

where $\kappa_0 \square \frac{1}{L_0}, \kappa_m \square \frac{1}{l_0}$, L_0 is the outer scale of turbulence, and l_0 is the inner scale of turbulence. Hence (46) becomes

$$\sigma_s^2 = 4(.033)\pi^2 k^2 L C_n^2 \int_0^\infty \frac{\kappa e^{-\frac{\kappa^2}{\kappa_m^2}}}{\left(\kappa^2 + \kappa_0^2\right)^{\frac{11}{6}}} d\kappa \tag{48}$$

To evaluate the integral we use the following identity [1]

$$\int \frac{\kappa^{2\mu} e^{-\frac{\kappa^2}{\kappa_m{}^2}}}{\left(\kappa^2+\kappa_0{}^2\right)^{\frac{11}{6}}} d\kappa = \frac{1}{2}\kappa_0{}^{2\mu-\frac{8}{3}}\Gamma\left(\mu+\frac{1}{2}\right)U\left(\mu+\frac{1}{2};\mu-\frac{1}{3};\frac{\kappa_0{}^2}{\kappa_m{}^2}\right) \tag{49}$$

where $U(a;b;x)$ is the confluent hypergeometric function of the second kind. Then from (49),

$$\int \frac{\kappa e^{-\frac{\kappa^2}{\kappa_m{}^2}}}{\left(\kappa^2+\kappa_0{}^2\right)^{\frac{11}{6}}} d\kappa = \frac{1}{2}\kappa_0{}^{-\frac{5}{3}}U\left(1;\frac{1}{6};\frac{\kappa_0{}^2}{\kappa_m{}^2}\right) \tag{50}$$

Note that $\frac{\kappa_0}{\kappa_m} = \frac{l_0{}^2}{L_0{}^2} < 1$. Consequently, we can replace the confluent hypergeometric function by its small argument asymptotic form. Using the small argument property associated with the confluent hypergeometric functions below,

$$U(a;c;z) \approx \frac{\Gamma(1-c)}{\Gamma(1+a-c)} + \frac{\Gamma(c-1)}{\Gamma(a)} z^{1-c}, |z| < 1 \tag{51}$$

we have

$$U(1;\frac{1}{6};\frac{\kappa_0^{\,2}}{\kappa_m^{\,2}}) \cong \frac{\Gamma\left(\frac{5}{6}\right)}{\Gamma\left(\frac{11}{6}\right)} + \frac{\Gamma\left(-\frac{5}{6}\right)}{\Gamma(1)}\left(\frac{\kappa_0^{\,2}}{\kappa_m^{\,2}}\right)^{\frac{5}{6}} \tag{52}$$

Then (50) reduces to

$$\int \frac{\kappa e^{-\frac{\kappa^2}{\kappa_m^{\,2}}}}{\left(\kappa^2+\kappa_0^{\,2}\right)^{\frac{11}{6}}} d\kappa \cong \frac{3}{5}\kappa_0^{\,-\frac{5}{3}} + \Gamma\left(-\frac{5}{6}\right)\kappa_m^{\,-\frac{5}{3}} \tag{53}$$

Because phase fluctuations are associated primarily with large turbulent scales, we can ignore inner scale effects. Hence if we take the limit as $l_0 \to 0\left(\kappa_m \to \infty\right)$, we obtain

$$\begin{aligned}\sigma_s^2 &= 4\left(\frac{0.033}{0.42}\right)\pi^2 k^2 L C_n^{\,2}\left(\frac{3}{5}\kappa_0^{\,-\frac{5}{3}} + \Gamma\left(-\frac{5}{6}\right)\kappa_m^{\,-\frac{5}{3}}\right) \\ &= 1.86\left(\frac{L_0}{r_0}\right)^{\frac{5}{3}},\end{aligned} \tag{54}$$

where $r_0 = \left(0.42 C_n^{\,2} k^2 L\right)^{-\frac{3}{5}}$ is Fried's parameter that describes the atmospheric coherence width. Larger values of r_0 correspond to "better seeing".

We will now compute the phase variance reduction associated with the different Zernike modes. The reduced or corrected variance is given by

$$\sigma_{s,corr}^2 = 4\pi^2 k^2 \int_0^L \int_0^\infty \kappa \phi_n(\kappa)\left\{1 - \sum_{\mathrm{j}=1}^{\mathrm{N}} F_{\mathrm{j}}(\kappa)\right\} d\kappa dz \tag{55}$$

Piston Removed:

The phase variance with the piston mode removed due to a finite aperture diameter D is

$$\begin{aligned}\sigma_{s,corr}^2 &= 4\pi^2 k^2 \int_0^L \int_0^\infty \kappa \phi_n(\kappa) \left\{ 1 - e^{-\frac{\kappa^2 D^2}{16}} \right\} d\kappa dz \\ &= 4\pi^2 k^2 \int_0^L \int_0^\infty \kappa \phi_n(\kappa) d\kappa dz - 4\pi^2 k^2 \int_0^L \int_0^\infty \kappa \phi_n(\kappa) e^{-\frac{\kappa^2 D^2}{16}} d\kappa dz\end{aligned} \tag{56}$$

which we write as

$$\sigma_{s,corr}^2 = 1.86 \left(\frac{L_0}{r_0} \right)^{\frac{5}{3}} - \sigma_{s,piston}^2 \tag{57}$$

where we have used the result in (54). The second integral in (56), $\sigma_{s,piston}^2$, involving the exponential function becomes

$$\int \frac{\kappa e^{-\frac{\kappa^2}{\kappa_m^2} - \frac{\kappa^2 D^2}{16}}}{\left(\kappa^2 + \kappa_0^2 \right)^{\frac{11}{6}}} d\kappa \cong \frac{3}{5} \kappa_0^{-\frac{5}{3}} + \frac{1}{2} \Gamma\left(-\frac{5}{6} \right) \frac{\left(1 + \frac{\kappa_m^2 D^2}{16} \right)^{\frac{5}{6}}}{\kappa_m^{\frac{5}{3}}} \tag{58}$$

where we have used the result of (53). Then

$$\int \frac{\kappa e^{-\frac{\kappa^2}{{\kappa_m}^2}}\left(1-e^{-\frac{\kappa^2 D^2}{16}}\right)}{\left(\kappa^2+{\kappa_0}^2\right)^{\frac{11}{6}}}d\kappa = \frac{3}{5}{\kappa_0}^{-\frac{5}{3}} + \frac{\Gamma\left(-\frac{5}{6}\right)}{{\kappa_m}^{\frac{5}{3}}} - \frac{3}{5}{\kappa_0}^{-\frac{5}{3}} - \frac{\Gamma\left(-\frac{5}{6}\right)\left(1+\frac{{\kappa_m}^2 D^2}{16}\right)^{\frac{5}{6}}}{{\kappa_m}^{\frac{5}{3}}} \tag{59}$$

Again we take the limit as $l_0 \to 0\left(\kappa_m \to \infty\right)$, from which we deduce

$$\int \frac{\kappa e^{-\frac{\kappa^2}{{\kappa_m}^2}}\left(1-e^{-\frac{\kappa^2 D^2}{16}}\right)}{\left(\kappa^2+{\kappa_0}^2\right)^{\frac{11}{6}}}d\kappa = -\Gamma\left(-\frac{5}{6}\right)\left(\frac{D^2}{16}\right)^{\frac{5}{6}} \tag{60}$$

Consequently, the piston-removed phase variance in (57) reduces to

$$\begin{aligned}\sigma^2_{s,corr} &= 1.86\left(\frac{L_0}{r_0}\right)^{\frac{5}{3}} - \left[1.86\left(\frac{L_0}{r_0}\right)^{\frac{5}{3}} - 1.02\left(\frac{D}{r_0}\right)^{\frac{5}{3}}\right] \\ &= 1.02\left(\frac{D}{r_0}\right)^{\frac{5}{3}}\end{aligned} \tag{61}$$

Tilt Removed:

Recall when computing the variance and piston-removed variance we saw that a singularity exists at $\kappa = 0$. Therefore, the von Karman spectrum, which is finite at the origin, was used for convergence of the integral. All other filters move the region of interest away from the origin. Hence we can now use the Kolmogorov spectrum which is given by

$$\phi_n(\kappa) = 0.033 {C_n}^2 \kappa^{-\frac{11}{3}} \tag{62}$$

The total tilt filter $F_{tilt}(\kappa)$ includes equal contributions from both x and y directions. The phase variance for removing the tilt effect is

$$\begin{aligned} \sigma_{s,tilt}^2 &= 4\pi^2 k^2 L \int_0^\infty \kappa \phi_n(\kappa) F_{tilt}(\kappa) d\kappa \\ &= 4\pi^2 k^2 L \int_0^\infty \kappa \phi(\kappa) \frac{\kappa^2 D^2}{16} e^{-\frac{\kappa^2 D^2}{16}} d\kappa \end{aligned} \tag{63}$$

Using the Kolmogorov spectrum gives us

$$\sigma_{s,tilt}^2 = 4\pi^2 k^2 L (.033 {C_n}^2) \frac{D^2}{16} \int_0^\infty \kappa \kappa^{-\frac{5}{3}} e^{-\frac{\kappa^2 D^2}{16}} d\kappa \tag{64}$$

which reduces to a Gamma function and further reduces to (See Appendix B)

$$\sigma_{s,tilt}^2 = 0.857 \left(\frac{D}{r_0} \right)^{\frac{5}{3}} \tag{65}$$

For $F_{tilt}(\kappa)$, the x and y directions have equal effect. Then after subtracting the phase effect from(61) , we have $\sigma_{s,corr}^2 = 0.592 \left(\frac{D}{r_0} \right)^{\frac{5}{3}}$ for the cosine portion and $\sigma_{s,corr}^2 = 0.164 \left(\frac{D}{r_0} \right)^{\frac{5}{3}}$ for the sine portion.

The phase variance for removing the effect of focus and astigmatism were obtained in a similar way (see Appendix B). They are

Focus removed:

$$\sigma_{s,corr}^2 = 0.129\left(\frac{D}{r_0}\right)^{\frac{5}{3}} \tag{66}$$

and

Astigmatism removed:

$$\sigma_{s,corr}^2 = 0.094\left(\frac{D}{r_0}\right)^{\frac{5}{3}} \tag{67}$$

In Table 4 expressions for σ_s^2 are shown for the first 6 Zernike modes, where D is the diameter of the circular aperture and r_0 is the atmospheric coherence length. Note that the greatest reduction in the variance $\sigma_{s,corr}^2$ of the piston-removed phase is due to Z_2 and Z_3, the tilt modes of the turbulence. Also, as i increases, the reduction in σ_s^2 which results from removing additional Zernike modes is small. The higher order Zernike modes make an additional small contribution to the residual mean square phase error.

Table 4 Removed phase variance σ_s^2 for Zernike modes from the turbulence-corrupted phase front

Mode index, i	Conventional	Gaussian Approximation
1	$1.03\left(\frac{D}{r_0}\right)^{\frac{5}{3}}$	$1.02\left(\frac{D}{r_0}\right)^{\frac{5}{3}}$
2	$0.582\left(\frac{D}{r_0}\right)^{\frac{5}{3}}$	$0.592\left(\frac{D}{r_0}\right)^{\frac{5}{3}}$
3	$0.134\left(\frac{D}{r_0}\right)^{\frac{5}{3}}$	$0.164\left(\frac{D}{r_0}\right)^{\frac{5}{3}}$
4	$0.111\left(\frac{D}{r_0}\right)^{\frac{5}{3}}$	$0.129\left(\frac{D}{r_0}\right)^{\frac{5}{3}}$
5	$0.088\left(\frac{D}{r_0}\right)^{\frac{5}{3}}$	$0.111\left(\frac{D}{r_0}\right)^{\frac{5}{3}}$
6	$0.065\left(\frac{D}{r_0}\right)^{\frac{5}{3}}$	$0.094\left(\frac{D}{r_0}\right)^{\frac{5}{3}}$

CHAPTER 8
ADAPTIVE OPTICS AND SCINTILLATION INDEX

Atmospheric turbulence causes phase variations in optical communication systems which are seen as random variations in intensity. Intensity fluctuations or scintillation is partially caused by phase variations due to the turbulent atmosphere. The scintillation index σ_I^2 is calculated from the parameters of the propagation path, the wavelength, and the spatial covariance function appropriately filtered for removal of aberration modes by the adaptive optics system. For all propagation paths the scintillation index is the normalized variance of the intensity. The scintillation index for a plane wave without adaptive optics known as the Rytov variance σ_I^2 is given by

$$\begin{aligned}\sigma_I^2 &= 8\pi^2 k^2 L \int_0^1 \int_0^\infty \kappa \phi_n(\kappa) \left[1 - \cos\frac{L\kappa^2 \xi}{k}\right] d\kappa d\xi \\ &= 1.23 C_n^2 k^{\frac{7}{6}} L^{\frac{11}{6}}\end{aligned} \tag{68}$$

where L = propagation path length and we have assumed C_n^2 is constant along the path.

8.1 Scintillation Reduction through Tilt Removal

By removing an increasing number of Zernike modes, we can assess the potential increase in performance of the optical system. Removing $N-1$ Zernike modes leads to

$$\sigma_{I,corrected}^2 = 8\pi^2 k^2 L \int_0^1 \int_0^\infty \kappa \phi_n(\kappa) \left[1 - \cos \frac{L\kappa^2 \xi}{k} \right] \left\{ 1 - \sum_{j=2}^{N} F_j(\kappa) \right\} d\kappa d\xi \qquad (69)$$

where $F_j(\kappa) =$ Zernike spatial filter function. If we split (69) into a difference of integrals, the first set of integrals are exactly $\sigma_I^{\,2}$ given by (68) and we are left with

$$\sigma_{I,corrected}^2 = \sigma_I^2 - 8\pi^2 k^2 L \int_0^1 \int_0^\infty \kappa \phi_n(\kappa) \sum_{j=2}^{N} F_j(\kappa) \left[1 - \cos \frac{L\kappa^2 \xi}{k} \right] d\kappa d\xi \qquad (70)$$

We start the summation in (69) with $j = 2$ since $j = 1$ corresponds to piston which is equivalent to aperture averaging due to a large collecting aperture of diameter D. The scintillation index with only tilt removed $j = 2$ is given by

$$\begin{aligned}
\sigma_{I,corrected}^2 &= 1.23 C_n^2 k^{\frac{7}{6}} L^{\frac{11}{6}} - \sigma_{I,tilt}^2 \\
&= 1.23 C_n^2 k^{\frac{7}{6}} L^{\frac{11}{6}} - 8\pi^2 k^2 L \int_0^1 \int_0^\infty \kappa \phi_n(\kappa) \left[1 - \cos \frac{L\kappa^2 \xi}{k} \right] F_2(\kappa) d\kappa d\xi \\
&= 1.23 C_n^2 k^{\frac{7}{6}} L^{\frac{11}{6}} - 8\pi^2 k^2 L \int_0^1 \int_0^\infty \kappa \phi_n(\kappa) \left[1 - \mathrm{Re}\left[\exp\left(-i \frac{L\kappa^2 \xi}{k} \right) \right] \right] \left[\frac{\kappa^2 D^2}{16} e^{-\frac{\kappa^2 D^2}{16}} \right] d\kappa d\xi \\
&= 1.23 C_n^2 k^{\frac{7}{6}} L^{\frac{11}{6}} - (I_1 - I_2)
\end{aligned} \qquad (71)$$

Looking at the first integral I_1 in the expression for tilt gives us

$$
\begin{aligned}
I_1 &= 8\pi^2 k^2 L \int_0^1 \int_0^\infty \kappa \phi_n(\kappa) \left[\frac{\kappa^2 D^2}{16} e^{-\frac{\kappa^2 D^2}{16}} \right] d\kappa d\xi \\
&= \frac{8\pi^2 0.033 C_n^{\ 2}}{16} k^2 L D^2 \int_0^1 \int_0^\infty \kappa^{-\frac{2}{3}} e^{-\frac{\kappa^2 D^2}{16}} d\kappa d\xi \\
&= 1.713 \left(\frac{D}{r_0} \right)^{\frac{5}{3}}
\end{aligned}
\tag{72}
$$

The second integral I_2 is computed in the same way as I_1. It is given by

$$
\begin{aligned}
I_2 &= 8\pi^2 k^2 L \int_0^1 \int_0^\infty \kappa \phi_n(\kappa) \operatorname{Re}\left[\exp\left(-i \frac{L\kappa^2 \xi}{k} \right) \right] \left[\frac{\kappa^2 D^2}{16} e^{-\frac{\kappa^2 D^2}{16}} \right] d\kappa d\xi \\
&= \frac{8\pi^2 .033 C_n^{\ 2}}{16} k^2 L D^2 \operatorname{Re} \int_0^1 \int_0^\infty \kappa^{-\frac{2}{3}} \exp\left[-\frac{\kappa^2 D^2}{16} \left(1 + i \frac{16 L \xi}{k D^2} \right) \right] d\kappa d\xi \\
&= 2.06 \left(\frac{D}{r_0} \right)^{\frac{5}{3}} \left\{ \frac{kD^2}{16L} \left[1 + \left(\frac{16L}{kD^2} \right)^2 \right]^{\frac{5}{12}} \right\} \sin\left(\frac{5}{6} \tan^{-1}\left(\frac{16L}{kD^2} \right) \right)
\end{aligned}
\tag{73}
$$

Hence the scintillation index after tilt removal is

$$
\begin{aligned}
\sigma_{I,corrected}^2 &= 1.23 C_n^2 k^{\frac{7}{6}} L^{\frac{11}{6}} - \sigma_{I,tilt}^2 \\
&= 1.23 C_n^2 k^{\frac{7}{6}} L^{\frac{11}{6}} \\
&\quad - 1.713 \left(\frac{D}{r_0} \right)^{\frac{5}{3}} \left\{ 1 - (1.20) \frac{kD^2}{16L} \left[1 + \left(\frac{16L}{kD^2} \right)^2 \right]^{\frac{5}{12}} \sin\left(\frac{5}{6} \tan^{-1}\left(\frac{16L}{kD^2} \right) \right) \right\}
\end{aligned}
\tag{74}
$$

8.2 Scintillation Reduction through Tilt and Focus Removal

The scintillation index with both tilt $j=2$ and focus $j=3$ removed is given by

$$\begin{aligned}
\sigma^2_{I,corrected} &= 1.23C_n^2 k^{\frac{7}{6}} L^{\frac{11}{6}} - \sigma^2_{I,tilt} - \sigma^2_{I,focus} \\
&= 1.23C_n^2 k^{\frac{7}{6}} L^{\frac{11}{6}} - \sigma^2_{I,tilt} \\
&\quad -8\pi^2 k^2 L \int_0^1 \int_0^\infty \kappa \phi_n(\kappa) \left[1 - \cos \frac{L\kappa^2 \xi}{k} \right] F_3(\kappa) d\kappa d\xi \\
&= 1.23C_n^2 k^{\frac{7}{6}} L^{\frac{11}{6}} - \sigma^2_{I,tilt} \\
&\quad -8\pi^2 k^2 L \int_0^1 \int_0^\infty \kappa \phi_n(\kappa) \left[1 - \mathrm{Re}\left[\exp\left(-i \frac{L\kappa^2 \xi}{k} \right) \right] \right] \left[\frac{\kappa^4 D^4}{1024} e^{-\frac{\kappa^2 D^2}{16}} \right] d\kappa d\xi \\
&= 1.23C_n^2 k^{\frac{7}{6}} L^{\frac{11}{6}} - \sigma^2_{I,tilt} - (I_1 - I_2)
\end{aligned} \tag{75}$$

The first integral I_1 in (75) gives us

$$\begin{aligned}
I_1 &= 8\pi^2 k^2 L \int_0^1 \int_0^\infty \kappa \phi_n(\kappa) \left[\frac{\kappa^4 D^4}{1024} e^{-\frac{\kappa^2 D^2}{16}} \right] d\kappa d\xi \\
&= \frac{8\pi^2 0.033 C_n^{\ 2}}{16} k^2 L D^4 \int_0^1 \int_0^\infty \kappa^{\frac{4}{3}} e^{-\frac{\kappa^2 D^2}{16}} d\kappa d\xi \\
&= 0.0714 \left(\frac{D}{r_0} \right)^{\frac{5}{3}}
\end{aligned} \tag{76}$$

The second integral I_2 is given by

$$
\begin{aligned}
I_2 &= 8\pi^2 k^2 L \int_0^1 \int_0^\infty \kappa \phi_n(\kappa) \operatorname{Re}\left[\exp\left(-i \frac{L\kappa^2 \xi}{k} \right) \right] \left[\frac{\kappa^4 D^4}{1024} e^{-\frac{\kappa^2 D^2}{16}} \right] d\kappa d\xi \\
&= \frac{8\pi^2 .033 C_n^{\ 2}}{1024} k^2 L D^2 \operatorname{Re} \int_0^1 \int_0^\infty \kappa^{\frac{4}{3}} \exp\left[-\frac{\kappa^2 D^2}{16} \left(1 + i \frac{16 L \xi}{k D^2} \right) \right] d\kappa d\xi \qquad (77) \\
&= 0.0714(6) \left(\frac{D}{r_0} \right)^{\frac{5}{3}} \left\{ \frac{kD^2}{16L} \left[1 + \left(\frac{16L}{kD^2} \right)^2 \right]^{-\frac{1}{12}} \right\} \sin\left(\frac{1}{6} \tan^{-1}\left(\frac{16L}{kD^2} \right) \right)
\end{aligned}
$$

Hence the scintillation index after tilt and focus removal is

$$
\begin{aligned}
\sigma^2_{I,corrected} &= 1.23 C_n^2 k^{\frac{7}{6}} L^{\frac{11}{6}} - \sigma^2_{I,tilt} - \sigma^2_{I,focus} \\
&= 1.23 C_n^2 k^{\frac{7}{6}} L^{\frac{11}{6}} - \sigma^2_{I,tilt} - \qquad (78) \\
&\quad - 0.0714 \left(\frac{D}{r_0} \right)^{\frac{5}{3}} \left\{ 1 - (6) \left\{ \frac{kD^2}{16L} \left[1 + \left(\frac{16L}{kD^2} \right)^2 \right]^{-\frac{1}{12}} \right\} \sin\left(\frac{1}{6} \tan^{-1}\left(\frac{16L}{kD^2} \right) \right) \right\}
\end{aligned}
$$

8.3 Graphical Results

Graphical results illustrate that filters derived using the Gaussian approximation gives a larger reduction of scintillation than the conventional filter (as seen in Figures 7-8). Also, we see the additional reduction in scintillation is small as more Zernike modes are removed

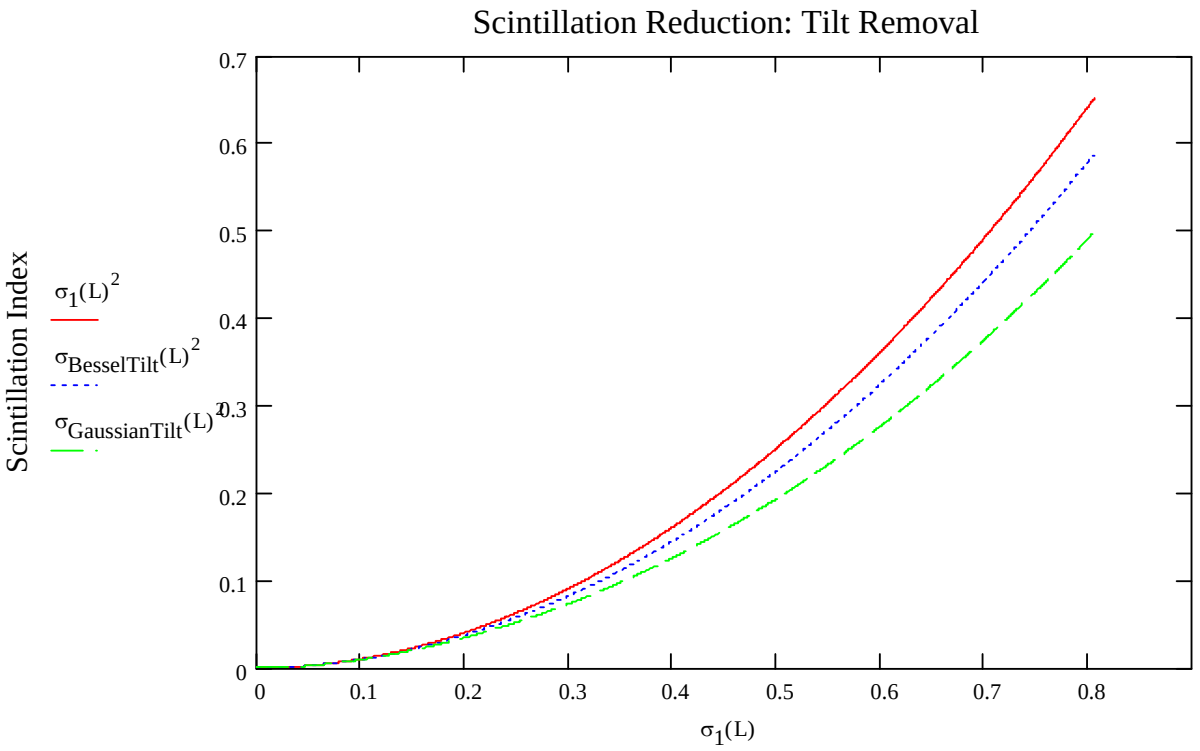

Figure 7 *Scintillation reduction using tilt removal only*

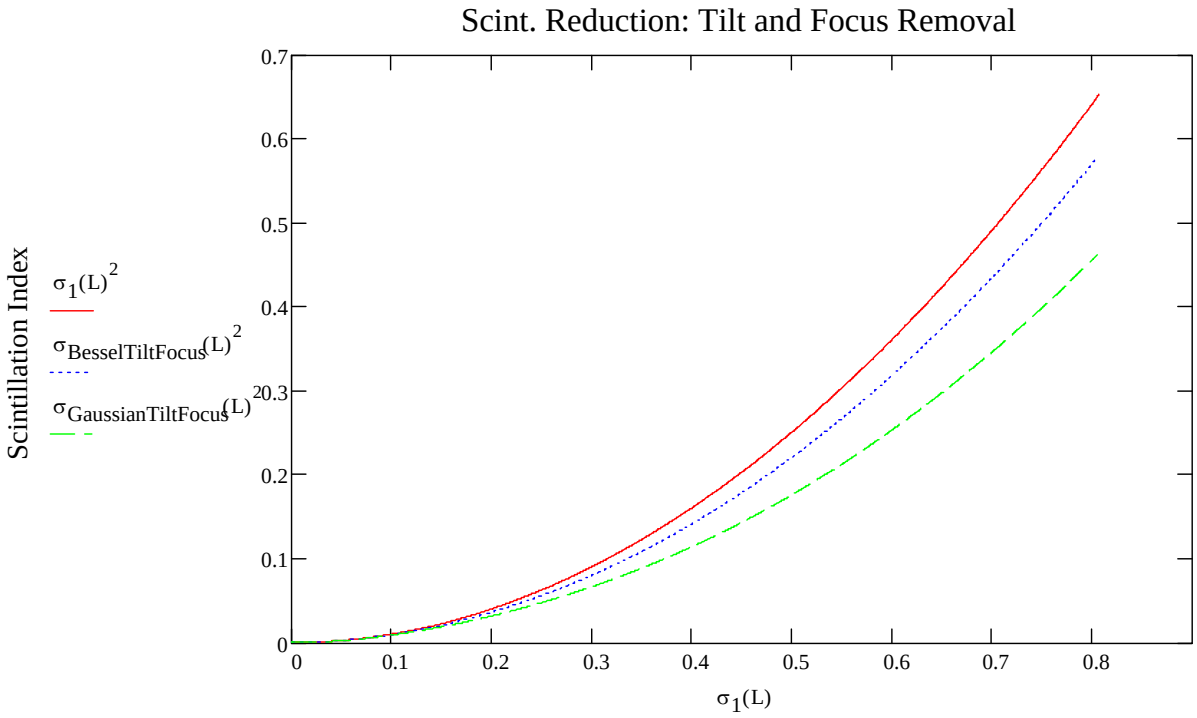

Figure 8 *Scintillation reduction using tilt and focus removal*

CHAPTER 9
SUMMARY

Gaussian approximation is a reasonable method for determining filter functions that can be used to remove lower order aberrations. Comparison with the conventional method for computing the filter functions demonstrates the validity of the Gaussian method in this application. Analysis of removed phase variance for Zernike modes from the turbulence-corrupted phase front (Table 4) demonstrated that results of the Gaussian method approximate those of the conventional method. A greater difference in what each method predicts is seen in higher-order Zernike modes

Comparison of the Gaussian and conventional methods also demonstrated several advantages of the Gaussian method. The Gaussian method leads to analytical expressions that can be applied to phase variance reduction and scintillation reduction. In scintillation reduction, the Gaussian method predicted greater reduction. It is not known at this time whether this is as good a model as that obtained by conventional analysis. Experimental results are not available to make such a comparison. Finally, although the Gaussian method is evaluated here using a plane wave, it can also be applied to spherical waves and Gaussian beam waves.

APPENDIX A
CALCULATIONS OF FILTER FUNCTIONS

In this appendix, more detail is provided for the calculation of the aperture filter functions.

Filter 1:

The first aperture filter function which represents the piston mode is defined by

$$G_1(\kappa,\phi)=\frac{1}{\pi}\int_0^{\infty}\int_0^{2\pi} e^{ir\kappa\cos(\theta-\phi)}Z_1(r,\theta)2e^{-2r^2}\,r\,d\theta\,dr \qquad (79)$$

Using the identity $\int_0^{2\pi} e^{ir\kappa\cos(\theta-\phi)}d\theta=2\pi J_0(\kappa r)$, $G_1(\kappa)$ reduces to

$$G_1(\kappa)=4\int_0^{\infty} re^{-2r^2}J_0(\kappa r)\,dr \qquad (80)$$

where $J_0(\kappa r)$ is the Bessel function of the first kind of order zero and is defined by

$$J_0(\kappa r)=\sum_{n=0}^{\infty}\frac{(-1)^n\left(\frac{\kappa r}{2}\right)^{2n}}{(n!)^2} \qquad (81)$$

Substituting (81) into the equation for $G_1(\kappa)$ gives us

$$G_1(\kappa)=4\sum_{n=0}^{\infty}\frac{(-1)^n\left(\frac{\kappa}{2}\right)^{2n}}{(n!)^2}\int_0^{\infty} r^{2n+1}e^{-2r^2}\,dr \qquad (82)$$

By letting $t = 2r^2$, $G_1(\kappa)$ reduces to

$$G_1(\kappa) = 4\sum_{n=0}^{\infty} \frac{(-1)^n \left(\frac{\kappa}{2}\right)^{2n}}{(n!)^2} \frac{1}{2^n} \int_0^{\infty} t^n e^{-t} dt$$
$$4\sum_{n=0}^{\infty} \frac{(-1)^n \left(\frac{\kappa}{2}\right)^{2n}}{(n!)^2} \frac{1}{2^n} \Gamma(n+1) \qquad (83)$$

Since $\Gamma(n) = \int_0^{\infty} t^{n-1} e^{-t} dt$.

To further simplify we use the property $\Gamma(n+1) = n!$ which leads to

$$G_1(\kappa) = 4\sum_{n=0}^{\infty} \frac{(-1)^n \left(\frac{\kappa^2}{8}\right)^n}{n!} \qquad (84)$$

which is the series representation for the exponential function or

$$G_1(\kappa) = e^{-\frac{\kappa^2}{8}} \qquad (85)$$

Therefore, the aperture filter function is given by

$$F_{piston} = e^{-\frac{\kappa^2}{4}} \qquad (86)$$

Filter 2:

The second filter is computed similarly and is used to remove tilt. It is defined by

$$G_2(\kappa,\phi) = \frac{1}{\pi}\int_0^{\infty}\int_0^{2\pi} e^{ir\kappa\cos(\theta-\phi)} Z_2(r,\theta) 2e^{-2r^2} r\,d\theta\,dr \\ \frac{1}{\pi}\int_0^{\infty}\int_0^{2\pi} e^{ir\kappa\cos(\theta-\phi)} 2r\cos\theta\, 2e^{-2r^2} r\,d\theta\,dr \tag{87}$$

Using the identity

$$e^{ir\kappa\cos(\theta-\phi)} = J_0(\kappa r) + 2\sum_{k=0}^{\infty} i^k J_k(\kappa r)\cos k(\theta-\phi) \tag{88}$$

Then

$$\int_0^{2\pi} e^{ir\kappa\cos(\theta-\phi)}\cos\theta\,d\theta = \int_0^{2\pi} J_0(\kappa r)\cos\theta\,d\theta + \int_0^{2\pi} 2\sum_{k=0}^{\infty} i^k J_k(\kappa r)\cos k(\theta-\phi)\cos\theta\,d\theta$$
$$= J_0(\kappa r)\int_0^{2\pi}\cos\theta\,d\theta + 2\sum_{k=0}^{\infty} i^k J_k(\kappa r)\cos k\phi\int_0^{2\pi}\cos k\theta\cos\theta\,d\theta \tag{89}$$
$$+ 2\sum_{k=0}^{\infty} i^k J_k(\kappa r)\sin k\phi\int_0^{2\pi}\sin k\theta\cos\theta\,d\theta$$

Hence we are left with

$$\int_0^{2\pi} e^{ir\kappa\cos(\theta-\phi)}\cos\theta\,d\theta = 2\pi i J_1(\kappa r)\cos\phi \tag{90}$$

In arriving at our result, we have used the identity $\cos(A-B)=\cos A\cos B+\sin A\sin B$ and the orthogonality properties $\int_0^{2\pi}\cos k\theta\cos n\theta=0, n\neq k$ and $\int_0^{2\pi}\cos k\theta\sin n\theta=0, all\ n\ and\ k$. Using the result in (90) $G_2(\kappa)$ simplifies to

$$G_2(\kappa)=8\int_0^{\infty}r^2e^{-2r^2}J_1(\kappa r)\cos\phi dr \qquad (91)$$

where $J_1(\kappa r)$ is the Bessel function of the first kind of order one and is defined by

$$J_1(\kappa r)=\sum_{n=0}^{\infty}\frac{(-1)^n\left(\frac{\kappa r}{2}\right)^{2n+1}}{n!(n+1)!} \qquad (92)$$

Substituting (92) into the equation for $G_1(\kappa)$ gives us

$$G_2(\kappa)=8i\sum_{n=0}^{\infty}\frac{(-1)^n\left(\frac{\kappa}{2}\right)^{2n+1}}{(n!)^2}\cos\phi\int_0^{\infty}r^{2n+3}e^{-2r^2}dr \qquad (93)$$

Using the definition of the Gamma function, $G_2(\kappa)$ reduces to

$$G_2(\kappa)=\frac{\kappa}{2}i\cos\phi e^{-\frac{\kappa^2}{8}} \qquad (94)$$

The y component for the tilt mode is derived using the same procedure and is defined by

$$G_3(\kappa) = \frac{\kappa}{2} i \sin\phi e^{-\frac{\kappa^2}{8}} \tag{95}$$

Taking the sum of the squared magnitudes gives us

$$\begin{aligned} F_{tilt}(\kappa) &= \left|G_2(\kappa)\right|^2 + \left|G_3(\kappa)\right|^2 \\ &= \frac{\kappa^2}{4} e^{-\frac{\kappa^2}{4}} \end{aligned} \tag{96}$$

for the total tilt effect.

Normalization for Gaussian Approximation:

$$C_3 = \frac{1}{\pi}\int_0^{\infty}\int_0^{2\pi} r2e^{-2r^2}(2A_3 r\sin\theta)^2 d\theta dr = 1$$
$$= \frac{2(A_3)^2}{\pi}\int_0^{\infty} r(4r^2)e^{-2r^2}dr\int_0^{2\pi}\sin^2\theta d\theta \qquad (97)$$
$$= 8(A_3)^2\int_0^{\infty} r^3 e^{-2r^2}dr = (A_3)^2 = 1$$

$$C_4 = \frac{1}{\pi}\int_0^{\infty}\int_0^{2\pi} r2e^{-2r^2}(\sqrt{3}A_4(2r^2-1)^2 d\theta dr = 1$$
$$= \frac{6(A_4)^2}{\pi}\int_0^{\infty} r(2r^2-1)e^{-2r^2}dr\int_0^{2\pi} d\theta \qquad (98)$$
$$= 3(A_4)^2 = 1 \Rightarrow (A_4)^2 = \frac{1}{3}$$

$$C_5 = \frac{1}{\pi}\int_0^{\infty}\int_0^{2\pi} r2e^{-2r^2}(\sqrt{6}A_5 r^2\cos\theta)^2 d\theta dr = 1$$
$$= \frac{12(A_5)^2}{\pi}\int_0^{\infty} r^5 e^{-2r^2}dr\int_0^{2\pi}\cos^2\theta d\theta \qquad (99)$$
$$= 12(A_5)^2 * \frac{1}{8} \Rightarrow (A_5)^2 = \frac{2}{3}$$

$$C_6 = \frac{1}{\pi}\int_0^{\infty}\int_0^{2\pi} r2e^{-2r^2}(\sqrt{6}A_6 r^2\sin\theta)^2 d\theta dr = 1$$
$$= \frac{12(A_6)^2}{\pi}\int_0^{\infty} r^5 e^{-2r^2}dr\int_0^{2\pi}\sin^2\theta d\theta \qquad (100)$$
$$= 12(A_6)^2 * \frac{1}{8} \Rightarrow (A_6)^2 = \frac{2}{3}$$

APPENDIX B
PHASE VARIANCE CALCULATIONS

In this appendix, more detail is provided for the calculation of each mode reduced phase variance.

Tilt-removed phase variance:

$$\begin{aligned}\sigma_{s,tilt}^2 &= 4\pi k^2 L\int_0^\infty \kappa\phi_n(\kappa)F_{tilt}(\kappa)d\kappa \\ &= 4\pi k^2 L\int_0^\infty \kappa\phi_n(\kappa)\frac{\kappa^2 D^2}{16}e^{-\frac{\kappa^2 D^2}{16}}d\kappa\end{aligned} \tag{101}$$

Substituting in the Kolmogorov spectrum give us

$$\begin{aligned}\sigma_{s,tilt}^2 &= 4\pi^2 k^2 L(.033C_n^{\ 2})\frac{D^2}{16}\int_0^\infty \kappa\kappa^{-\frac{5}{3}}e^{-\frac{\kappa^2 D^2}{16}}d\kappa \\ &= 4\pi^2 k^2 L(.033C_n^{\ 2})\frac{D^2}{16}\left\{3\Gamma\left(\frac{7}{6}\right)\left(\frac{16}{D^2}\right)^{\frac{1}{6}}\right\}\end{aligned} \tag{102}$$

Then we have

$$\sigma_{s,tilt}^2 = 0.857\left(\frac{D}{r_0}\right)^{\frac{5}{3}} \tag{103}$$

For $F_{tilt}(\kappa)$, the x and y directions have equal effect. Then after subtracting the phase effect from(61), we have $\sigma_{s,corr}^2 = 0.592\left(\frac{D}{r_0}\right)^{\frac{5}{3}}$ for the cosine portion and $\sigma_{s,corr}^2 = 0.164\left(\frac{D}{r_0}\right)^{\frac{5}{3}}$ for the sine portion

Focus-removed phase variance:

$$\begin{aligned}\sigma_{s,focus}^2 &= 4\pi k^2 L\int_0^\infty \kappa\phi_n(\kappa)F_{focus}(\kappa)d\kappa \\ &= 4\pi k^2 L\int_0^\infty \kappa\phi_n(\kappa)\frac{\kappa^4 D^4}{1024}e^{-\frac{\kappa^2 D^2}{16}}d\kappa\end{aligned} \quad (104)$$

Substituting in the Kolmogorov spectrum gives us

$$\begin{aligned}\sigma_{s,focus}^2 &= 4\pi^2 k^2 L(.033C_n^{\ 2})\frac{D^2}{16}\int_0^\infty \kappa\kappa^{\frac{1}{3}}e^{-\frac{\kappa^2 D^2}{16}}d\kappa \\ &= 4\pi^2 k^2 L(.033C_n^{\ 2})\frac{D^4}{1024}\left\{\frac{1}{2}\Gamma\left(\frac{7}{6}\right)\left(\frac{16}{D^2}\right)^{\frac{7}{6}}\right\}\end{aligned} \quad (105)$$

Then the phase effect for the focus mode is

$$\sigma_{s,focus}^2 = 0.035\left(\frac{D}{r_0}\right)^{\frac{5}{3}} \quad (106)$$

and the focus-removed phase variance is given by

$$\sigma_{s,corr}^2 = 0.129\left(\frac{D}{r_0}\right)^{\frac{5}{3}} \quad (107)$$

Astigmatism-removed phase variance:

The phase variance for astigmatism is calculated using the same phase reduction integral as that for focus given by (104) since the aperture filter functions are equal. However, as with $F_{tilt}(\kappa)$, the x and y directions have equal effect for astigmatism. Therefore, the phase effect $\sigma^2_{s,astig} = 0.035\left(\frac{D}{r_0}\right)^{\frac{5}{3}}$ gives us $\sigma^2_{s,corr} = 0.111\left(\frac{D}{r_0}\right)^{\frac{5}{3}}$ for the cosine portion and $\sigma^2_{s,corr} = 0.094\left(\frac{D}{r_0}\right)^{\frac{5}{3}}$ for the sine portion

APPENDIX C
SCINTILLATION REDUCTION CALCULATIONS

In this appendix, additional steps are provided for calculation of the scintillation reduction with tilt removal and reduction with tilt and focus removal.

Tilt-reduced scintillation:

The scintillation index with only tilt removed $j = 2$ is given by

$$\begin{aligned}\sigma^2_{I,corrected} &= 1.23C_n^2 k^{\frac{7}{6}} L^{\frac{11}{6}} - 8\pi^2 k^2 L \int_0^1 \int_0^\infty \kappa \phi_n(\kappa) \left[1 - \cos\frac{L\kappa^2\xi}{k}\right] F_2(\kappa) d\kappa d\xi \\ &= 1.23C_n^2 k^{\frac{7}{6}} L^{\frac{11}{6}} - 8\pi^2 k^2 L \int_0^1 \int_0^\infty \kappa \phi_n(\kappa) \left[1 - \mathrm{Re}\left[\exp\left(-i\frac{L\kappa^2\xi}{k}\right)\right]\right]\left[\frac{\kappa^2 D^2}{16} e^{-\frac{\kappa^2 D^2}{16}}\right] d\kappa d\xi \quad (108) \\ &= 1.23C_n^2 k^{\frac{7}{6}} L^{\frac{11}{6}} - (I_1 - I_2)\end{aligned}$$

Looking at the first integral I_1 in the expression for tilt gives us

$$\begin{aligned} I_1 &= 8\pi^2 k^2 L \int_0^1 \int_0^\infty \kappa \phi_n(\kappa) \left[\frac{\kappa^2 D^2}{16} e^{-\frac{\kappa^2 D^2}{16}}\right] d\kappa d\xi \\ &= \frac{8\pi^2 0.033 C_n^{\ 2}}{16} k^2 L D^2 \int_0^1 \int_0^\infty \kappa^{-\frac{2}{3}} e^{-\frac{\kappa^2 D^2}{16}} d\kappa d\xi \quad (109) \\ &= 1.713\left(\frac{D}{r_0}\right)^{\frac{5}{3}} \end{aligned}$$

The second integral I_2 is computed in the same way as I_1. It is given by

$$\begin{aligned} I_2 &= 8\pi^2 k^2 L \int_0^1 \int_0^\infty \kappa \phi_n(\kappa)\, \mathrm{Re}\left[\exp\left(-i\frac{L\kappa^2\xi}{k}\right)\right]\left[\frac{\kappa^2 D^2}{16} e^{-\frac{\kappa^2 D^2}{16}}\right] d\kappa d\xi \\ &= \frac{8\pi^2 .033 C_n^{\ 2}}{16} k^2 L D^2\, \mathrm{Re} \int_0^1 \int_0^\infty \kappa^{-\frac{2}{3}} \exp\left[-\frac{\kappa^2 D^2}{16}\left(1 + i\frac{16L\xi}{kD^2}\right)\right] d\kappa d\xi \end{aligned} \quad (110)$$

Taking only the integral with respect to κ, we have

$$\int_0^\infty \kappa^{-\frac{2}{3}} \exp\left[-\frac{\kappa^2 D^2}{16}\left(1+i\frac{16L\xi}{kD^2}\right)\right] d\kappa = \frac{3\Gamma(\frac{7}{6})}{\left[\frac{D^2}{16}\left(1+i\frac{16L\xi}{kD^2}\right)\right]^{\frac{1}{6}}} \tag{111}$$

$$= \left(\frac{16}{D^2}\right)^{\frac{1}{6}} 3\Gamma(\frac{7}{6})\left(1+i\frac{16L\xi}{kD^2}\right)^{-\frac{1}{6}}$$

Substituting back into (110) give us

$$I_2 = \frac{8\pi^2 .033 C_n^{\ 2}}{32} k^2 L D^{\frac{5}{3}} 16^{\frac{1}{6}} \Gamma\left(\frac{1}{6}\right) \mathrm{Re} \int_0^1 \left(1+i\frac{16L\xi}{kD^2}\right)^{-\frac{1}{6}} d\xi$$

$$= \frac{3\pi^2 .033 C_n^{\ 2}}{10} k^2 L D^{\frac{5}{3}} 16^{\frac{1}{6}} \Gamma\left(\frac{1}{6}\right) \mathrm{Re}\left[\frac{kD^2}{16iL}\left(1+i\frac{16L}{kD^2}\right)^{\frac{5}{6}} - \frac{kD^2}{16iL}\right] \tag{112}$$

$$= 2.06\left(\frac{D}{r_0}\right)^{\frac{5}{3}} \left\{\frac{kD^2}{16L}\left[1+\left(\frac{16L}{kD^2}\right)^2\right]^{\frac{5}{12}}\right\} \sin\left(\frac{5}{6}\tan^{-1}\left(\frac{16L}{kD^2}\right)\right)$$

Hence the scintillation index after tilt removal is

$$\sigma^2_{I,corrected} = 1.23 C_n^2 k^{\frac{7}{6}} L^{\frac{11}{6}} - \sigma^2_{I,tilt}$$

$$= 1.23 C_n^2 k^{\frac{7}{6}} L^{\frac{11}{6}} \tag{113}$$

$$-1.713\left(\frac{D}{r_0}\right)^{\frac{5}{3}} \left\{1-(1.20)\frac{kD^2}{16L}\left[1+\left(\frac{16L}{kD^2}\right)^2\right]^{\frac{5}{12}} \sin\left(\frac{5}{6}\tan^{-1}\left(\frac{16L}{kD^2}\right)\right)\right\}$$

Tilt and focus-reduced scintillation:

The scintillation index with both tilt $j=2$ and focus $j=3$ removed is given by

$$\begin{aligned}
\sigma_{I,corrected}^2 &= 1.23C_n^2 k^{\frac{7}{6}} L^{\frac{11}{6}} - \sigma_{I,tilt}^2 - \sigma_{I,focus}^2 \\
&= 1.23C_n^2 k^{\frac{7}{6}} L^{\frac{11}{6}} - \sigma_{I,tilt}^2 \\
&\quad -8\pi^2 k^2 L \int_0^1 \int_0^\infty \kappa \phi_n(\kappa) \left[1 - \cos \frac{L\kappa^2 \xi}{k} \right] F_3(\kappa) d\kappa d\xi \\
&= 1.23C_n^2 k^{\frac{7}{6}} L^{\frac{11}{6}} - \sigma_{I,tilt}^2 \\
&\quad -8\pi^2 k^2 L \int_0^1 \int_0^\infty \kappa \phi_n(\kappa) \left[1 - \mathrm{Re}\left[\exp\left(-i \frac{L\kappa^2 \xi}{k} \right) \right] \right] \left[\frac{\kappa^4 D^4}{1024} e^{-\frac{\kappa^2 D^2}{16}} \right] d\kappa d\xi \\
&= 1.23C_n^2 k^{\frac{7}{6}} L^{\frac{11}{6}} - \sigma_{I,tilt}^2 - (I_1 - I_2)
\end{aligned} \tag{114}$$

The first integral I_1 in (75) gives us

$$\begin{aligned}
I_1 &= 8\pi^2 k^2 L \int_0^1 \int_0^\infty \kappa \phi_n(\kappa) \left[\frac{\kappa^4 D^4}{1024} e^{-\frac{\kappa^2 D^2}{16}} \right] d\kappa d\xi \\
&= \frac{8\pi^2 0.033 C_n^{\ 2}}{16} k^2 L D^4 \int_0^1 \int_0^\infty \kappa^{\frac{4}{3}} e^{-\frac{\kappa^2 D^2}{16}} d\kappa d\xi \\
&= 0.0714 \left(\frac{D}{r_0} \right)^{\frac{5}{3}}
\end{aligned} \tag{115}$$

The second integral I_2 is computed in the same way as I_1. It is given by

$$\begin{aligned} I_2 &= 8\pi^2 k^2 L \int_0^1 \int_0^\infty \kappa \phi_n(\kappa) \operatorname{Re}\left[\exp\left(-i \frac{L\kappa^2 \xi}{k} \right) \right] \left[\frac{\kappa^2 D^2}{16} e^{-\frac{\kappa^2 D^2}{16}} \right] d\kappa d\xi \\ &= \frac{8\pi^2 .033 C_n^{\ 2}}{16} k^2 L D^2 \operatorname{Re} \int_0^1 \int_0^\infty \kappa^{\frac{4}{3}} \exp\left[-\frac{\kappa^2 D^2}{16} \left(1 + i \frac{16 L \xi}{k D^2} \right) \right] d\kappa d\xi \end{aligned} \tag{116}$$

Taking only the integral with respect to κ we have

$$\begin{aligned} \int_0^\infty \kappa^{\frac{4}{3}} \exp\left[-\frac{\kappa^2 D^2}{16} \left(1 + i \frac{16 L \xi}{k D^2} \right) \right] d\kappa &= \frac{1}{2} \Gamma(\frac{7}{6}) \left[\frac{D^2}{16} \left(1 + i \frac{16 L \xi}{k D^2} \right) \right]^{-\frac{7}{6}} \\ &= \left(\frac{16}{D^2} \right)^{\frac{7}{6}} \Gamma(\frac{7}{6}) \left(1 + i \frac{16 L \xi}{k D^2} \right)^{-\frac{7}{6}} \end{aligned} \tag{117}$$

Substituting back into (110) give us

$$\begin{aligned} I_2 &= \frac{8\pi^2 .033 C_n^{\ 2}}{32} k^2 L D^{\frac{5}{3}} 16^{\frac{7}{6}} \Gamma\left(\frac{1}{6} \right) \operatorname{Re} \int_0^1 \left(1 + i \frac{16 L \xi}{k D^2} \right)^{-\frac{7}{6}} d\xi \\ &= \frac{3\pi^2 .033 C_n^{\ 2}}{10} k^2 L D^{\frac{5}{3}} 16^{\frac{7}{6}} \Gamma\left(\frac{1}{6} \right) \operatorname{Re} \left[6 \frac{k D^2}{16 i L} \left[1 - \left(1 + i \frac{16 L}{k D^2} \right)^{-\frac{1}{6}} \right] \right] \\ &= 0.0714(6) \left(\frac{D}{r_0} \right)^{\frac{5}{3}} \left\{ \frac{k D^2}{16 L} \left[1 + \left(\frac{16 L}{k D^2} \right)^2 \right]^{-\frac{1}{12}} \right\} \sin\left(\frac{1}{6} \tan^{-1}\left(\frac{16 L}{k D^2} \right) \right) \end{aligned} \tag{118}$$

Hence the scintillation index after tilt and focus removal is

$$\begin{aligned}\sigma^2_{I,corrected} &= 1.23C_n^2k^{\frac{7}{6}}L^{\frac{11}{6}} - \sigma^2_{I,tilt} - \sigma^2_{I,focus} \\ &= 1.23C_n^2k^{\frac{7}{6}}L^{\frac{11}{6}} - \sigma^2_{I,tilt} - \\ &\quad -0.0714\left(\frac{D}{r_0}\right)^{\frac{5}{3}}\left\{1-(6)\left\{\frac{kD^2}{16L}\left[1+\left(\frac{16L}{kD^2}\right)^2\right]^{-\frac{1}{12}}\right\}\sin\left(\frac{1}{6}\tan^{-1}\left(\frac{16L}{kD^2}\right)\right)\right\}\end{aligned} \quad (119)$$

REFERENCES

[1] Andrews, L.C. and Phillips, R.L. (2005). *Laser Beam Propagation through Random Media* (2nd edition). Bellingham, Washington: SPIE Press.

[2] Andrews, L.C. and Phillips, R.L. (2003). *Mathematical Techniques for Engineers and Scientists.* Bellingham, Washington: SPIE Press.

[3] Noll, R. J. (1976). Zernike polynomials and atmospheric turbulence. *J. Opt. Soc. Am., 66,* 207-211.

[4] Wikimedia Foundation, Inc. (2006). *Wikipedia, the free encyclopdia.* Aug 12, 2006, http://en.wikipedia.org/wiki/Main_Page.

[5] University of California. (2006). *Center for Adaptive Optics.* Sept. 19, 2005, http://cfao.ucolick.org

[6] Encyclopedia Britannica. (2006). *atmospheric turbulence -- Encyclopedia Britannica Online.* Sept. 30, 2006, http://www.britannica.com/eb/article-9010124

[7] Association of Universities for Research in Astronomy, Inc. (2001). *NOAO.* Sept. 19, 2005, http://www.ctio.noao.edu/

[8] Craig Mackay and the Lucky Imaging Team. (2006). *Atmospheric Turbulence.* Sept. 30, 2006, http://www.ast.cam.ac.uk/~optics/Lucky_Web_Site/LI_Atmos_Turb.htm

[9] Roggemann, M.C. and Welsh, B. (1996). *Imaging Through Turbulence.* Boca Raton, Florida: CRC Press.